

# Magneto-thermal instabilities in $\kappa$ -(BEDT-TTF)<sub>2</sub>Cu(NCS)<sub>2</sub>

M. M. Mola and S. Hill<sup>†</sup>

*Department of Physics, Montana State University, Bozeman, MT 59717*

J. S. Brooks and J. S. Qualls

*Department of Physics and National High Magnetic Field Laboratory, Florida State University, Tallahassee, FL 32310*

(November 21, 2018)

Angle and temperature dependent torque magnetization measurements are reported for the organic superconductor  $\kappa$ -(ET)<sub>2</sub>Cu(NCS)<sub>2</sub>, at extremely low temperatures ( $\sim T_c/10^3$ ). Magneto-thermal instabilities are observed in the form of abrupt magnetization (flux) jumps. We carry out an analysis of the temperature and field orientation dependence of these flux jumps based on accepted models for layered type-II superconductors. Using a simple Bean model, we also find a critical current density of  $4 \times 10^8$  A.m<sup>-2</sup> from the remnant magnetization, in agreement with previous measurements.

*Keywords:* superconductivity, vortices, critical state

## 1. Introduction

Since the discovery of highly anisotropic high- $T_c$  superconductors (HTS) and organic superconductors, there has been a renewed interest in magneto-thermal instabilities within the mixed superconducting state [1,2,3]. Much of this interest derives from the limit such instabilities could potentially place on technological applications. Our recent work has shown that much of the field-temperature ( $\mathbf{B}, T$ ) phase diagram for the organic superconductor  $\kappa$ -(ET)<sub>2</sub>Cu(NCS)<sub>2</sub> is either within the quasi-two-dimensional (Q2D) vortex solid phase, or the vortex liquid state [4]. Thus, we can expect the rigidity of the Q2D pancake vortex solid to play an important role throughout much of the available mixed state  $\mathbf{B}, T$  phase diagram. To this end, we have used angle and temperature dependent torque magnetometry to investigate the mechanism by which magnetic flux enters an extreme type-II layered organic superconductor, and the instabilities caused in the process.

## 2. Experimental

A capacitive cantilever torque magnetometer was used to detect changes in the magnetization of a single crystal of  $\kappa$ -(ET)<sub>2</sub>Cu(NCS)<sub>2</sub>, with approximate dimensions of  $1.0 \times 1.0 \times 0.3$  mm<sup>3</sup>. The torque beam and the sample were mounted on a single axis rotator, allowing for angle dependent measurements. An angle  $\theta = 0^\circ$  refers to the applied field aligned with the least conductive  $a$ -axis, while  $\theta = 90^\circ$  refers to the field parallel to the highly conducting  $bc$ -planes. Magnetization was obtained by dividing the measured torque by  $\mathbf{H}_{app} \times \sin \theta$ , and the volume of the sample, where  $\mathbf{H}_{app}$  is the applied field strength. Measurements were carried out at the National High Magnetic Field Laboratory using a <sup>3</sup>He/<sup>4</sup>He dilution refrigerator in conjunction with a 20 tesla super-

conducting magnet. The applied field was swept at a constant rate of 0.5 tesla per minute.

## 3. Results and Discussion

In Fig. 1, we plot magnetization vs. applied magnetic field for both up and down sweeps (signified with arrows), at 25 mK, and for angles between  $16.2^\circ$  and  $70.1^\circ$ . The magnetization initially increases on the up sweeps, reaches a maximum, and then decreases steadily until it reaches zero at the irreversibility field  $\mathbf{H}_{irr}$ ; the down sweeps exhibit similar behavior with the sign of the magnetization inverted. Catastrophic flux jumps are seen as a series of saw tooth oscillations superimposed upon the steadily decreasing magnetization curve. Between the flux jumps, the magnetization increases monotonically with field, with a slope proportional  $1/\mathbf{H}_{app}$  (see right inset to Fig. 1). We note that none of the flux jumps are complete, *i.e.* the magnetization minimum after a given jump never reaches zero. This implies that the flux gradient and associated critical currents are never totally dissipated, and the system is always in a metastable state. Notice also that the limiting magnetization values fall within a slowly varying (on the scale of the flux jumps) envelope, consistent with previous measurements on this material [3] as well as the HTS [1,2]. Moreover, hysteresis in the jump amplitudes in the up and down sweeps is observed; the down sweeps show smaller, more frequent flux jumps than the up sweeps, indicating that flux from a smaller volume of the crystal is participating in each jump [1].

In the right inset to Fig. 1, we plot  $dM/d\mathbf{H}_{app}$  vs.  $1/\mathbf{H}_{app}$  for  $\theta = 74.6^\circ$ . At low values of  $1/\mathbf{H}_{app}$ ,  $dM/d\mathbf{H}_{app}$  is small and constant. This is followed by a sudden increase to a field dependent value, which increases linearly with respect to  $1/\mathbf{H}_{app}$ . We find this slope to be a monotonically decreasing function of angle,

as can be seen in the left inset to Fig. 1. The dark, vertical streaks in the right inset correspond to the derivative taken over the discontinuities at the flux jumps, which appear as inverted delta functions. Note also that the average jump amplitude,  $A(\theta)$  (the difference in magnetization just before and after the discontinuity), is an increasing function of angle, which approximately follows a  $1 - \cos(\theta)$  dependence. This behavior is due to the quasi two dimensional (Q2D) nature of the material, *i.e.* the flux density scales as the cosine of the angle between the applied field and the direction normal to the superconducting planes [4].

Temperature dependent measurements were made between 25 and 200 mK, and at angles of  $47.7^\circ$  and  $74.6^\circ$ . Both angles gave qualitatively similar results, which can then be scaled to  $\theta = 0^\circ$  [4,5]. In Fig. 2, we plot magnetization for both up and down sweeps, at an angle of  $\theta = 47.7^\circ$ , and for temperatures of 87, 110, and 130 mK; each set of sweeps has been offset for clarity. Notice that the jumps get progressively larger and that the number of jumps decreases as the temperature increases.

It has previously been suggested [3] that flux jump behavior observed at dilution refrigerator temperatures can be attributed to a thermal Kapitza resistance which isolates the sample from the surrounding cryogen bath, thereby triggering runaway thermal instabilities. Due to the Kapitza resistance having a  $1/T^3$  dependence [6] and, therefore, a  $T^3$  thermal conductivity, the cryogen bath is able to remove heat (caused by flux flow) from the sample more efficiently at higher temperatures. Dissipation within the crystal arises due to the viscous flow of vortices into (out of) the sample as  $\mathbf{H}_{app}$  is increased (decreased). Power dissipation is, therefore, proportional to the square of the critical screening current density integrated over the volume of the crystal, *i.e.*  $q(J_c) \propto \int J_c^2 dV$ ;  $q(J_c)$  also depends on the rate at which flux enters the sample (the sweep rate), as has been demonstrated in earlier work [3]. As the temperature is increased, the cryogen bath is able to remove heat from the sample at a greater rate (power), which allows a larger integrated current to build up before any instability occurs. Hence the flux jumps are observed less frequently, and with greater magnitude, as the temperature is increased. We note that the magnetization is proportional to the curl of the critical screening current density integrated over the volume of the crystal, *i.e.*  $\mathbf{M} = \int (\nabla \times \mathbf{J}_c) dV$ , thus,  $\mathbf{M} \propto q^{1/2}$ . Therefore, it is not surprising that we observe the amplitude of the flux jumps to scale with temperature as  $\Delta \mathbf{M} \propto T^{3/2}$ . We believe that the sudden cessation of the flux jumps above a characteristic field  $\mathbf{B}_m(T)$ , which decreases upon increasing the temperature, is due to a Q2D melting transition (see Ref. [4]).

As seen above, the amount of dissipation depends on the sample volume through which screening currents flow. Thus, with a greater capacity for heat removal to the cryogen bath, currents will flow in a larger volume

of the crystal at higher temperatures, causing more flux to participate in each jump, *i.e.* larger, less frequent instabilities. We also notice that, as the temperature is increased, the jumps become more complete, indicating that there is less remnant current within the crystal following each instability.

Finally, using a simple Bean model [7], we use the remnant magnetization to determine the in-plane critical current for  $\kappa-(\text{ET})_2\text{Cu}(\text{NCS})_2$ . In Fig. 2, we label the magnetic field axis at the point where the magnetization equals zero on the up sweep. This point corresponds to equal numbers of vortices and anti-vortices within the sample, and is given by  $\mathbf{H}^* = 1/2 J_{c\parallel} d$ , where  $d$  is the diameter of the sample. Using  $d \sim 1$  mm, and  $\mathbf{H}^*$  scaled by the method mentioned above [5], we obtain an in-plane critical current density of,  $J_{c\parallel} \sim 4 \times 10^8$  A.m $^{-2}$ , in very good agreement with previous studies using other methods [8].

#### 4. Conclusions

We have used torque magnetometry to investigate the temperature and field orientation dependence of magneto-thermal instabilities in an organic superconductor. We find that the amplitude of the observed flux jumps – hence the number of vortices participating in each jump – is an increasing function of angle. We also find that the amplitude of the flux jumps increases with temperature as  $A \propto T^{3/2}$ , consistent with accepted models. Finally, we obtain an in-plane critical current density of  $J_{c\parallel} \sim 4 \times 10^8$  A.m $^{-2}$ , also consistent with previous measurements.

#### 5. Acknowledgements

This work was supported by the National Science Foundation (DMR-0071953), Research Corporation, and the Office of Naval Research (N00014-98-1-0538). Work carried out at the NHMFL was supported by a cooperative agreement between the State of Florida and the NSF under DMR-9527035.

---

<sup>†</sup> email: hill@physics.montana.edu

- [1] M. Guillot, M. Potel, P. Gougeon, H. Noel, J. C. Levet, G. Chouteau, J. L. Tholence, Phys. Lett. A **127**, 363 (1988).
- [2] A. Gerber, J. N. Li, Z. Tarnawski, J. J. M. Franse, A. A. Menovsky, Phys. Rev. B **47**, 6047 (1993).
- [3] A. G. Swanson, J. S. Brooks, H. Anzai, K. Konoshita, M. Tokumoto, K. Murata, Solid State Comm. **73**, 353 (1990).
- [4] M. M. Mola, S. Hill, J. S. Qualls, J. S. Brooks, cond-mat/0008262.
- [5] G. Blatter, M. V. Fiegl'man, G. Geshkenbein, A. I. Larkin, V. M. Vinokur, Rev. Mod. Phys. **66**, 1125 (1994).

[6] A. Kent, *Experimental Low-Temperature Physics*, AIP, New York, 1993.  
 [7] C. P. Bean, *Rev. Mod. Phys.* **36**, 31 (1964).

[8] M. M. Mola, J. T. King, C. P. McRaven, S. Hill, J. S. Qualls, J. S. Brooks, *Phys. Rev. B* **62**, 5965 (2000), and references therein.

**Figures**

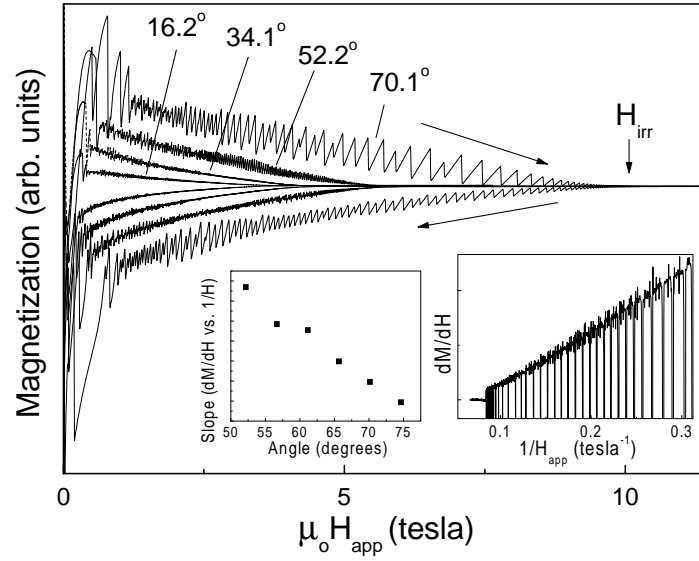


FIG. 1. Magnetization vs. magnetic field at 25 mK, for various angles  $\theta$ . The direction of the field sweeps is indicated by arrows. Right inset:  $d\mathbf{M}/d\mathbf{H}_{app}$  vs.  $1/\mathbf{H}_{app}$  shows linear slope above an initial jump. Left inset: Slope of  $d\mathbf{M}/d\mathbf{H}_{app}$  vs.  $1/\mathbf{H}_{app}$  (right inset) as a function of  $\theta$ .

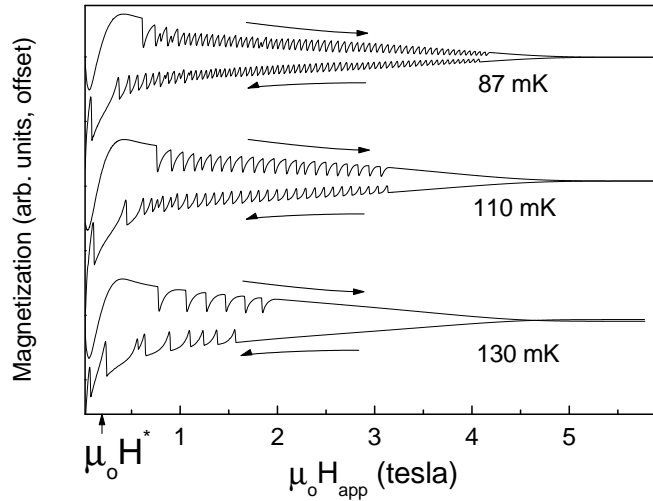


FIG. 2. Magnetization vs. applied magnetic field at an angle  $\theta = 47.7^\circ$ ; the sweep direction is indicated with arrows.  $\mathbf{H}^*$  is the full penetration field in Bean's model [7].